# Development of Concept Illustration Variants of the JUMP Lander


**Robert L. Howard, Jr., Ph.D.**
**NASA Johnson Space Center**
**2101 NASA Parkway, Mail Code SF3**
**Houston, TX 77058**
**robert.l.howard@nasa.gov**

**Nehemiah Williams, Ph.D.**
**NASA Johnson Space Center**
**2101 NASA Parkway, Mail Code EX-2**
**Houston, TX 77058**
**nehemiah.j.williams@nasa.gov**

**Sarosh Nandwani**
**NASA Johnson Space Center**
**2101 NASA Parkway, Mail Code SF3**
**Houston, TX 77058**
**sarosh.nandwani@nasa.gov**



*Abstract*— **The Artemis program is committed to landing humans on the Moon in the 2020s leading to a sustainable lunar presence by the end of the decade. It is challenging to deliver heavy payloads to the lunar surface in support of these goals given currently available Earth launch systems. The payload capacity of the launch systems limits the size of the lunar landers, thereby limiting their cargo capacity. Fortunately, lander cargo capacity can be significantly increased if multiple landers are joined together in space. This concept has been previously introduced as the Joinable Undercarriage to Maximize Payload (JUMP) Lander. Utilizing a JUMP Lander system will increase options and make it easier to comply with directives issued by senior White House leadership to initiate long duration human activity on the Moon. Such activity, by definition, implies extensive habitation, mobility, research, and resource development capability that in turn calls for significant mass delivery to the lunar surface. This paper develops three concept illustration variants of the JUMP Lander. These concepts explore hypergolic, hydrogen, and methane propellant options, as well as the power and thermal rejection systems necessary to enable such lander concepts. The paper also estimates masses for the necessary avionics, structures, and mechanical subsystems. The paper documents the resulting configurations and recommends a JUMP Lander to carry forward in further development.**


## TABLE OF CONTENTS



## 1. INTRODUCTION

*NASA Artemis Program*

Since the final Apollo landing in 1972, there have been repeated studies to return to the Moon. However, for the first time there are now commercial contracts in place for lunar landers. The NASA Artemis program is making steady progress towards humans on the Moon in 2024 with three crew lander contractors, [1] and the NASA Science Mission Directorate has already contracted four robotic precursor missions to the Moon with launches starting in June 2021. [2],[3],[4]

*Value of Heavy Payload Delivery*

However, a choke point for those who envision large scale lunar utilization is the payload capacity of lunar landers under development. Except for the Space X Starship, which requires parking orbit propellant transfer, [5] none of the commercial landers in development have publicly announced payload capacities significantly greater than the 14.5-ton capacity of the NASA Altair lunar lander [6] initiated under the previous Constellation program, which was cancelled in 2010. This cargo capacity potentially limits lunar development to much smaller, modular elements and prohibits large-diameter habitats such as the SLS-derived Common Habitat [7] which could mass in excess of 30 tons. [8]

*JUMP Lander Overview*

The JUMP Lander (short for Joinable Undercarriage to Maximize Payload) is a concept [9] that enables delivery of a roughly 30-ton payload to the lunar surface. The JUMP Lander is composed of multiple, identical core stages that are launched separately and assembled in space prior to mating with a lunar surface payload. A core stage is for all practical terms a lunar lander, generally sized to the mass and volume limits of the launch vehicle(s) intended to deliver it to space. The JUMP concept joins multiple lunar landers together in parallel, producing a resulting lander with order of magnitude increases in payload capacity.

*JUMP Lander Definitions, Constraints, and Assumptions*

Definitions

Cargo Launch Vehicle (CLV) will refer in this paper specifically to rockets in the "heavy" class produced by US corporations and available for US government missions. Examples include Delta IV Heavy, Atlas V, Falcon Heavy, New Glenn, and Vulcan. It does not include smaller rockets such as the Falcon 9 or Antares, nor larger rockets such as the Starship.

Constraints and Assumptions

This lander study is constrained to the use of CLVs for launch of JUMP lander core stages. Lander payloads are not subject to this constraint. This distinction recognizes that launch availability for CLVs is substantially greater (and at lower cost) than for SLS.

CLV launch availability is assumed to constrain JUMP core stages to launches separated by ten to eighteen days.

A CLV can delivery a payload of roughly 15 tons to Cislunar space.

The JUMP Core Stage must be compatible with at least three different CLV providers.

*Lander Trade Space*

Several key subsystem design trades can have significant impact on lander performance. These include propulsion, power, and thermal subsystems. Three conceptual landers will be developed based on these options, creating a trade space to identify a recommended lander configuration to represent the JUMP Lander concept.

## 2. TRADE SPACE DEFINITION

*Propellant Trade Space*

One of the defining factors of a lunar lander is the choice of propellant. The selection of a propellant type significantly drives lander dimensions and performance. While there are numerous options for propellant, three of the most popular types involve the fuels of liquid hydrogen, liquid methane, and hydrazine. These three fuels form the basis of the JUMP Lander trade space. The JUMP Lander will only consider chemical rockets, thus each of these fuels is associated with an oxidizer.

Liquid hydrogen fuel typically is combined with liquid oxygen (LOX). The LOX-Hydrogen combination is a very efficient chemical rocket propellant solution with the highest specific impulse among comparable chemical systems. Additionally, LOX and hydrogen are compatible with future goals for in-situ resource utilization (ISRU) on both the Moon and Mars as both bodies are known to have sources of water. However, both LOX and liquid hydrogen are cryogenic, requiring cryocoolers to prevent or slow boiloff. LOX has a boiling point of 90.19 K (-218.8°C) and liquid hydrogen has a boiling point of 20.28 K (-252.9°C). Hydrogen also has a very low density resulting in large propellant tanks as compared to similar masses of other fuels.

Liquid methane is also typically combined with LOX. Methane has a boiling point just above that of LOX, 111.7 K (-161.5°C), making it much easier to store for long durations in a propellant tank than liquid hydrogen. Methane is also compatible with ISRU goals for Mars, though it is not clear how readily sources of carbon can be found on the Moon to enable methane ISRU on the Moon. (Some carbon dioxide may be found in permanently shadowed craters at the lunar poles from cometary impacts, possibly establishing a resource for lunar methane production.)

Hypergolic propellants such as hydrazine have as an advantage that they do not require igniters – the fuel and oxidizer ignite on contact. They are also liquid at normal spacecraft temperatures. The specific form of hydrazine compared in this paper is monomethyl hydrazine (MMH). It can be combined with either nitrogen tetroxide or nitric acid. For this trade MMH will be used with MON-3, a mixture of 97% nitrogen tetroxide and 3% nitric acid. This is the formulation that was used in the Space Shuttle Orbital Maneuvering System (OMS) engine. Because hypergolic propellants ignite on contact, they are highly reliable. However, they have a lower specific impulse than cryogenic propellants and they are toxic, requiring elaborate ground handling operations.

*Main Engine Trade Space*

LOX-Hydrogen Engine

The RL-10 has been in use in various forms since 1963. [10] The use of liquid oxygen and liquid hydrogen propellants gives the RL-10 ideal thrust and specific impulse performance.

The variant in the JUMP Lander trade space is the RL-10-B2, which is currently flown on the Delta IV rocket. It has a mass of 301.19 kg and provides 110,271 N (24,790 lbf) thrust with a specific impulse of 465.5 seconds. The engine has a stowed length of 2.2 m (86.5 in), a deployed length of 4.15 m (163.5 in), and a nozzle diameter of 2.15 m (84.5 in).

LOX-Methane Engine

The candidate main engine for a LOX-Methane configuration is the prototype Morpheus engine developed at NASA Johnson Space Center. This engine was flown in several low-altitude tests in Texas and Florida. The HD4 configuration of the engine attained a thrust of 24,020.4 N (5400 lbf) [11] and a specific impulse of 321 seconds. [12]

MMH-MON-3 Engine

The AJ10-190 has been used on spacecraft and upper stages including the Vanguard, Delta, Titan, Apollo Service Module, Space Shuttle Orbital Maneuvering System, and Orion Service Module. The engine provides roughly 26,690 N (6000 lbf) thrust with a 316 second specific impulse. It is gimballed and can be steered ±7°. It has a mass of 118 kg. [13]

*RCS Thruster Trade Space*

In order to avoid the mass costs of a separate propellant system, reaction control system (RCS) thrusters will use the same propellant as the main engine, drawing from the same tanks.

LOX-Hydrogen Thrusters

For the case of LOX-Hydrogen, there are no flown examples of an oxygen-hydrogen thruster, but several have been tested over the past two decades. An example of a small thruster is the lateral thruster referenced in the Integrated Vehicle Fluids concept being developed by United Launch Alliance. [14]

The IVF lateral thruster uses gaseous oxygen and gaseous hydrogen drawn from the spacecraft's LOX and liquid hydrogen tanks and heated within the IVF system before reaching the thruster. The thruster achieves a thrust of 44.48-155.69 N (10-35 lbf). It can also operate in a cold gas mode by only commanding a hydrogen inlet valve open, enabling precision maneuvers in proximity to other vehicles. The IVF lateral thruster uses mixture ratios between 1 and 4 and the thruster has an $I_{sp}$ in excess of 350 seconds. This system is of course low TRL but enables commonality with a highly efficient main propulsion system and would provide excellent maneuverability for core stage docking operations. Unfortunately, no mass for this thruster is indicated in available literature, so the mass is being estimated as the average of three comparable performance hypergolic thrusters: MR-107T 110N, R-1E, and AJ10-220 [15], with an additional mass to represent the igniter, sized at three times the mass of a standard automotive spark plug. The resulting thruster mass is 1.91 kg.

A higher thrust example is the "workhorse" LOX/LH2 thruster developed by TRW (now Northrop Grumman) and tested at NASA Marshall Space Flight Center in 2002. [16] This thruster achieves a thrust of (1000 lbf) with a mixture ratio of 4. The specific impulse is 350 seconds. It is capable of operating in a low thrust mode producing (25 lbf). [16] An illustration of the engine is shown in Figure 1. The reference does not indicate a mass for this thruster. Consequently, the mass is estimated based on a linear scaling of the thrust to engine mass ratios for the similar performance hypergolic R-40 and R-40B engines plus an additional 0.6 kg to account for the igniter, resulting in a mass of 12.47 kg.

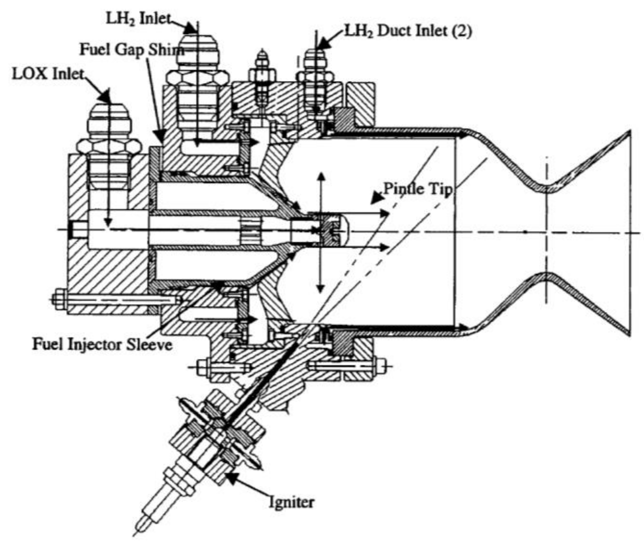

Figure 1. LOX/LH2 Workhouse Thruster

LOX-Methane Thrusters

Aerojet developed an 870-lbf (3870 N) thruster for both ethanol and methane fuels, shown in Figure 2. Similar to the TRW LOX-LH2 thruster it also has a 25-lbf dual mode [17]. Mass values for the thruster were not published. It is likely similar in mass to the Aerojet R-40 870-lbf hypergolic thruster and that value of 10.5 kg, plus 0.6 kg for an igniter, will be used.

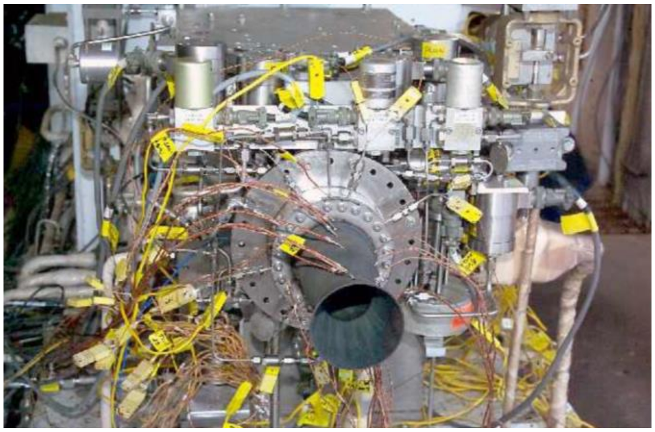
Figure 2. 870-lbf LOX/CH4 Thruster Undergoing Testing

Based on test data from the 870-lb thruster, Aerojet also developed a 100-lbf thruster, shown in Figure 3, achieving a 317-second $I_{sp}$ in test firings. [17] In the absence of published mass data, this paper will use as a placeholder the average of four variants [15] of the Aerojet R-4D 100-lbf hypergolic thruster, resulting in a thruster mass estimate of 4.68 kg.

Figure 3. 100-lbf LOX/CH4 Thruster

NASA Johnson Space Center developed a small LOX-Methane thruster, shown in Figure 4. as part of the Morpheus project and flew the thruster in multiple Morpheus low altitude test flights, both at Johnson and Kennedy Space Centers. The Morpheus thruster has an $I_{sp}$ of 233 seconds and a thrust of 80 N (18 lbf). It uses a 0.46 mixture ratio and has a mass of 1.36 kg. It has an oxygen mass flow rate of 0.015 kg/s and a methane mass flow rate of 0.034 kg/s. [18] For a flight system, the Morpheus team anticipated adding an expander nozzle, shown in Figure 5. Mass values for the nozzle added to the flight thruster were not published. Consequently, this study will assume a total RCE mass of 2.36 kg, assuming a 1 kg expander nozzle.

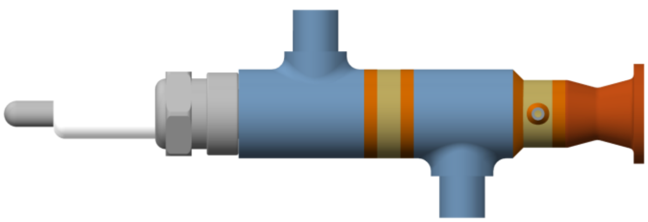

Figure 4. Morpheus Reaction Control Engine.

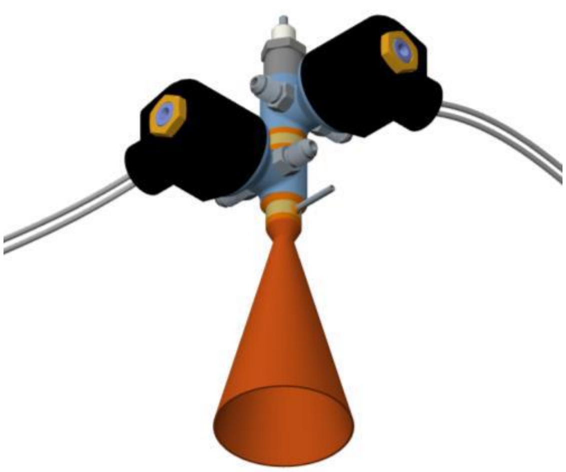

Figure 5. Morpheus Reaction Control Engine Space Concept

MMH-MON-3 Thrusters

The Space Shuttle Obiter's primary RCS thruster was the Aerojet R-40. The R-40B, shown in Figure 6, is no longer in production but is cited as a potential RCS engine for the JUMP Lander. It attains a thrust of 4000 N (900 lbf) with a 293-second specific impulse and a mass of 10.5 kg.

Figure 6. R-40B Bipropellant Rocket Engine

The R-4D is one of the most iconic RCS thrusters in existence. It was used on the Apollo Service Module and Lunar Module and is currently used on the H-II and ATV ISS cargo vehicles. There are several variants of the engine and the one to be considered for the JUMP Lander is the R-4D-11 with a 300:1 expansion ratio, shown in Figure 7. It has a thrust of 490 N (110 lbf) and a specific impulse of 315 seconds. It has a mass of 4.31 kg. [15]

Figure 7. R-4D-11 with 300:1 Expansion Ratio

*Power Trade Space*

An initial sizing estimate of 10 kW is assumed for the core stage power requirement. This is inclusive of power to operate all core stage systems as well as provide power to the payload.

The maximum eclipse period assumed for Cislunar parking orbits available to the core stage is 9.75 hours and the minimum daylight period is 146.25 hours. Energy storage systems will be sized based on a 9.75-hour eclipse period and 146.25 hours to recharge energy storage systems.

Nuclear power was initially considered as a possible option for the JUMP Lander. A NASA Kuiper Belt Object Orbiter design study used a 10 kWe nuclear fission reactor that was attractive from a reactor mass and power level [19] but it is not as viable for the JUMP Lander as it is for the Kuiper Belt Object Orbiter.

An advantage of the fission system is it easily provides continuous, stable power needed by the core stages while they loiter in Cislunar space awaiting the arrival of subsequent stages and the payload. Eclipse periods are irrelevant to such a system, eliminating the need for an energy storage system. It can also operate through dynamic flight periods and with no moving parts it is highly reliable.

However, these advantages are more than offset by its liabilities. It can take up to six hours to reach full power [20], meaning a secondary power source is required. Additionally, the reactor generates 43 kW of thermal energy [21] that must be rejected, necessitating a large radiator. Further, the reactor shield provided an 11.7° half-angle coverage, mounted on a 12.66-meter truss. This was sufficient for the Kuiper Belt Object Orbiter and could encompass virtually all of the spacecraft. But the JUMP Lander is a much larger vehicle and it along with its lunar surface payload would require a much larger shield. Distancing the reactor from the lander by using a truss on a high thrust vehicle would also be problematic. Consequently, nuclear power is not an option for the JUMP Lander.

Fuel cells provide an energy storage option for the JUMP Lander. Fuel cell options include alkaline fuel cells, proton-exchange membrane fuel cells, regenerative fuel cells, and solid oxide fuel cells. NASA has extensive flight history with alkaline fuel cells, which were flown on the Space Shuttle. [22] Proton-exchange membrane fuel cells promise higher power at lower mass with increased reliability. [23] Solid oxide fuel cells use easier to transport fuels than hydrogen but have the disadvantage of operating at high temperatures. [23] Regenerative fuel cells are composed of either alkaline or proton-exchange membrane fuel cells, but an electrolyzer then breaks the water into oxygen and hydrogen, allowing the process to be repeated. [23] The JUMP Lander will trade regenerative fuel cells as they can be used during eclipse periods and dynamic flight and be electrolyzed at other times.

Batteries are a possible source of energy storage and have been used on spacecraft since the beginning of the space program. Lithium-ion batteries represent the current high TRL state of the art. The JUMP Lander will trade the same battery system used on the International Space Station. The LSE134 lithium-ion battery has a rated capacity of 134 Ah, 3.7 V, and a mass of 3.53 kg per cell. Each cell measures 130x50x263 mm. [24]

The final power option to be traded is also a constant fixture of space power systems – solar power. Among the most capable solar systems are the Z4J Germanium quadruple junction solar cells produced by SolAero with an efficiency rating of approximately 30%. [25] These cells are slated to fly on the Gateway Power and Propulsion Element. [26]

*Thermal Trade Space*

Heat is transferred from spacecraft components through fluid loops to a radiator where it is rejected to the space environment. It is at this point that the JUMP Lander will explore different options. The radiator system may be body mounted or mounted on an articulating structure. It may also be fixed in place or it may deploy at some point after launch. The JUMP Lander will trade three radiator configurations: wing-mounted radiators, body mounted radiators plus fixed radiator fins, and body mounted telescoping radiators.

## 3. Trade Study Allocation to Concept Illustration Variants

The subsystem trades will be allocated across three variants to illustrate the JUMP Lander concept. All three will be sized at a high level and applied to a heavy cargo delivery scenario.

*Concept Illustration Variant 1*

Concept Illustration Variant 1 is a LOX-LH2 lander with solar array wings, regenerative fuel cells, and radiator wings. This variant represents the highest performance approach and emphasizes use of high TRL components.

Propulsion

The lander propellant tanks are sized based on the maximum amount of propellant mass that the CLV can deliver to Cislunar space. Each has an inner diameter of 4 meters, with 0.4-meter-tall (including insulation) elliptical domes. Barrel height is sized according to propellant mass, resulting in a total tank height of 2.14 meters for the liquid hydrogen tank and 1.03 meters for the liquid oxygen tank. Tank thickness, including pressure vessel wall, MLI, and other insulation, is estimated at 10 centimeters. The liquid oxygen tank is mounted on an intertank which rests on top of the liquid hydrogen tank.

The propellent system uses a Cryogenic Boil-off Reduction System (CBRS) for liquid hydrogen that combines active cooling with a passive thermal control system [27] to achieve a lower mass thermal control system than an equivalent performance passive system. [27] The liquid oxygen is maintained with an identical cryocooler to the active cooling system in the CBRS. Zero boil-off is achievable for liquid oxygen as 90K cryocoolers have been demonstrated in zero boil-off mode. [28]

A single RL-10-B2 is mounted directly beneath the liquid hydrogen tank. The primary RCS consists of twenty-four of the TRW/Northrop Grumman 1000-lbf "workhorse" thrusters [16] configured in eight three-jet modules, four mounted to the forward skirt and four mounted to the aft skirt. Four thrusters fire in each axis: ±x, ±y, and ±z. Sixteen United Launch Alliance IVF lateral thrusters [14] serve as vernier RCS. Four thrusters fire in the ±x axis and two thrusters fire in the ±y and ±z axes.

Power

Power generation is provided by an articulating solar array wing. The arrays must produce 17.4 kW to supply payload power, core stage operational power, and electrolyzer power. At the 30% efficiency claimed by the vendor SolAero [25], an inherent degradation coefficient of 0.77, and an average solar incidence angle of 30°, the solar array surface area is sized at approximately 65 m2, which is met in a single 4-meter by 16.25-meter array wing, a little more than twice the size of each of ESA's 2-meter by 7.3-meter Orion Service Module solar array wings. [29] Assuming similar structural reinforcement as the Orion wings, the JUMP core stage solar array wing can be expected to mass roughly 150 kg. The solar array wing is jettisoned just prior to powered descent.

Fuel cells will provide electrical power during eclipse periods, during descent and landing, and post-landing until reactant exhaustion. The Space Shuttle alkaline fuel cell, shown in Figure 8, is a placeholder solution for the JUMP core stage fuel cell. The shuttle fuel cell produces 7 kW continuous power and 12 kW peak power. [30] It measures 0.36 x 0.38 x 1.14 meters with a mass of 118 kg. [31] Each JUMP core stage will carry two fuel cells.

Water produced by the fuel cells will be stored in a holding tank for electrolysis. A commercial electrolyzer is used as a placeholder solution for the JUMP core stage. The QLC-1000 PEM Electrolyzer Cell Stack is approximately 0.138 meters in diameter and has a power consumption of 320 watts. [32] Six of these electrolyzers are needed to electrolyze enough water during non-eclipse periods.

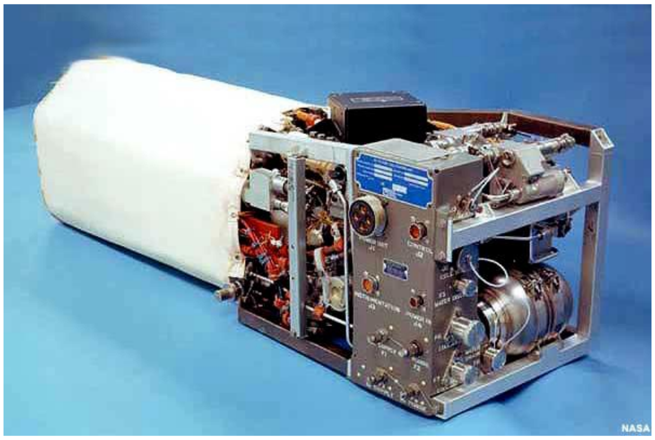

Figure 8. Space Shuttle Alkaline Fuel Cell

Fuel cells will initially draw reactants directly from the propulsion system. Gaseous oxygen and hydrogen produced by the electrolyzer will be stored in tanks until needed.

Thermal

The JUMP active thermal control system is derived from counterpart systems on the International Space Station and the initial US Service Module design for the Orion Multi-Purpose Crew Vehicle (MPCV). It consists of an ISS-derived Pump Flow Control Subassembly (PFCS), ammonia coolant, coldplates, and a radiator. The PFCS contains pumps, valves, and controls and performs the task of circulating the ammonia through the system. It measures 101.6 cm x 73.7 cm x 48.3 cm and masses 106.7 kg. [33]

An aluminum radiator wing with the same AZ-93 coating [34] identified for use in the body-mounted radiator panels on the Orion MPCV US Service Module rejects the heat it receives from the PFCS. Based on an emissivity of 0.9 [34] and a 14.9 kW heat rejection, a simple sizing tool approximates a radiator surface area of 36.04 $m^2$ [35] with a mass of 432.54 kg. The radiator is two-sided, with dimensions of 4 meters by 4.5 meters.

The radiator wing is mounted on the same articulating structure as the solar array wing, perpendicular to the solar array on the eclipse side of the solar array. Thus, as the solar array articulates to track the sun, the radiator is always perpendicular to the sun and in shadow, maximizing the heat rejection.

The radiator is jettisoned with the solar array wing just prior to descent. Heat rejection is provided during powered flight through a coolant loop that exchanges heat with propellant feed lines.

*Concept Illustration Variant 2*

Concept Illustration Variant 2 is a LOX-CH4 lander with solar array wings, batteries, and body-mounted and telescoping radiators. This variant explores the impact of a Mars-focused propellant architecture.

Propulsion

In the case of the LOX-Methane lander, the propellant tanks retain the same 4-meter diameter and 0.4-meter dome height, but the methane tank is only 1.03 meters tall and the oxygen tank is only 0.86 meters tall. The difference from the LOX-Hydrogen lander tank size is the difference in mixture ratio, the higher density methane, and heavier spacecraft subsystems leaving less mass available for propellant. Zero boil off cryocoolers are included in each tank. The same system of intertank, forward skirt, and aft skirt is employed in this lander variant.

Two Morpheus HD4 engines are mounted beneath the liquid methane tank. Twenty-four Aerojet 870-lbf methane thrusters provide primary RCS while sixteen Morpheus reaction control engines (RCEs) provide vernier RCS. The thruster configuration is identical to that of the hydrogen lander.

Power

Power generation is by means of the same solar power system used for Concept Illustration Variant 1 but the array sizing reflects the different power needs of Concept Illustration Variant 2. The key differences in power are driven by the replacement of the hydrogen CBRS with a duplicate of the oxygen cryocooler for the methane, and the use of batteries instead of a fuel cell. This results in a slightly lower power of 16.4 kW. The array wing measures 4 meters by 14.7 meters with an estimated mass of 140 kg.

Power during eclipse periods and landing is provided by batteries. Based on the previously mentioned LSE134 lithium ion battery and a depth of discharge of 80%, a total of 268 cells are required to store the required 146.66 kWh. This battery system occupies 0.46 $m^3$ and masses 946.04 kg.

Thermal

The same heat rejection system as employed for Concept Illustration Variant 1 is used, but is configured as a body mounted, telescoping system. The AZ-93 coated aluminum radiator is composed of three half-cylindrical panels, with the main panel mounted on the side of the intertank and liquid methane tank. The main panel measures 4.4 meters in diameter with an actual width of 6.9 meters and 3.29 meters in height. A second panel telescopes downward from it, measuring 3.14 meters in height. A third panel telescopes downward from the second, measuring 2.57 meters in height. A notional representation of the radiator is shown in Figure 9 and Figure 10. The effective surface area of the radiator is 39.62 $m^2$ with an estimated mass of 475.49 kg.

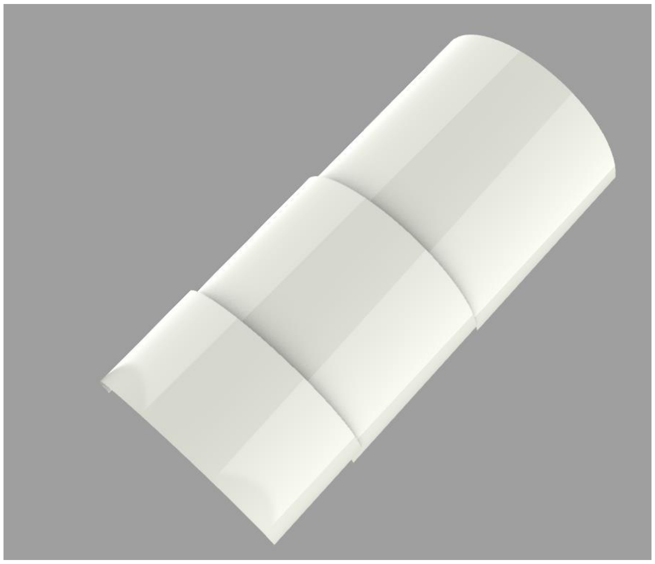

Figure 9. Telescoping Radiator Panels (Deployed)

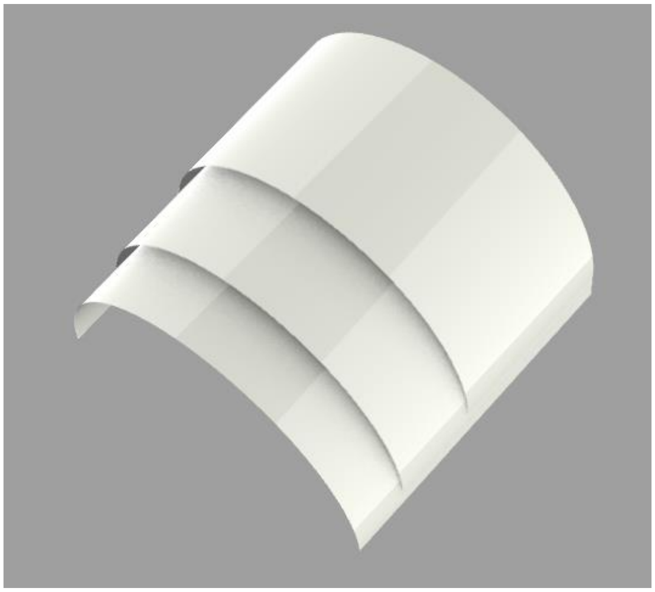

Figure 10. Telescoping Radiator Panels (Stowed)

*Concept Illustration Variant 3*

Concept Illustration Variant 3 is a MMH-MON-3 lander with solar array wings, batteries, body-mounted radiators, and radiator fins. This variant emphasizes long-duration in-space storability and emphasizes use of high TRL components.

Propulsion

The hypergolic propellant tanks are the smallest, as those are the highest density propellants in this trade study. Both tanks have a diameter of 3.82 meters with dome heights of 0.288 meters. The tanks are all dome and do not have barrel sections. Unlike the hydrogen and methane landers, monomethyl hydrazine and MON-3 are liquid at nominal temperatures.

Two AJ10-190 engines are mounted to the base of the hydrazine tank. Primary RCS consists of twenty-four Aerojet R-40B thrusters and vernier RCS consists of sixteen Aerojet R-4D-11 thrusters, both in the same configuration as the hydrogen and methane landers.

Power

The hypergolic propulsion system does not require cryocoolers, thus reducing lander power requirements to 13.6 kW. The resulting solar array wing measures 4 meters by 12.2 meters with an estimated mass of 120 kg.

The LSE134 lithium ion batteries provide power during eclipse and landing, with 223 cells providing 97.5 kWh. The batteries occupy 0.38 $m^3$ with a mass of 787.19 kg.

Thermal

Heat rejection is provided by a combination of a fixed body-mounted radiator and two radiator fins. Both utilize the AZ-93 coated aluminum radiator panels previously discussed.

The body-mounted radiator is similar to the main panel used by Concept Illustration Variant 2, with a slightly stretched height of 3.35 meters. Based on a 13.6 kW heat rejection, the radiator surface area is 32.93 $m^2$ with an estimated mass of 395.13 kg. Each fin is mounted at the edge of the radiator panel perpendicular to the panel surface, as shown in Figure 11, and shares the same height of 3.35 meters with a width of 2.71 meters. The fins can articulate up to 50 degrees to avoid intersecting with the fins of other core stages in the mated configuration, though this does cause a loss of heat rejection performance.

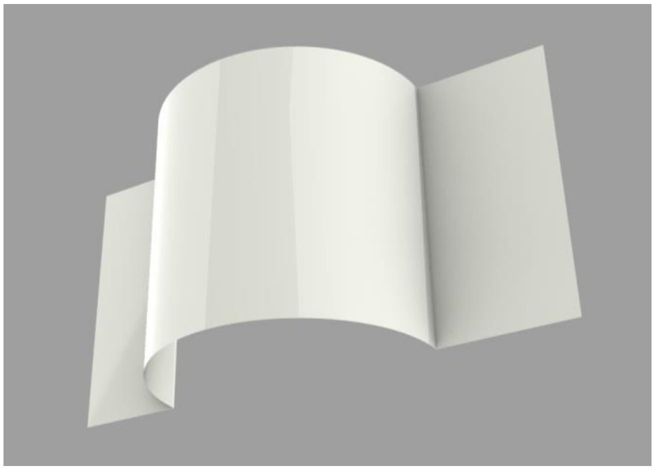

Figure 11. Body-Mounted Radiator with Fins

## 4. Non-Traded Subsystem Sizing for Concept Illustration Variants

Some subsystems will not be directly sized for the JUMP Lander concept illustration variants. The three variants are primarily denoted by their propulsion systems (LOX-LH2, LOX-CH4, and MMH/N2O4) and power systems (solar, battery, and fuel cell).

*Avionics*

The Command and Data Handling (C&DH) subsystem, Communications and Tracking (C&T) subsystem, and Guidance, Navigation, and Control (GN&C) subsystem are all identical across all three variants and are not influenced in any way by the propulsion and power system trades. Thus, there is no value gained for purposes of this study by defining a specific implementation.

In order to account for their masses in JUMP Lander sizing, average values are computed for each subsystem using internal NASA pre-Artemis space vehicle studies to provide placeholder values. This provides values with a basis in realism.

The communications system provides direct comm to Earth with the Earth-Moon L2 as the furthest distance for sizing purposes. Both RF and optical systems are potential options. It provides communication for both the lander and payload. Once all core stages are docked together and docked to the payload, only one lander core stage is likely to have line of sight to Earth at any given time, thus the communications system must support the bandwidth of all core stages and the payload. This includes high resolution photo and video, in addition to telemetry for all elements. It may also serve as a relay for surface assets immediately following landing, up through payload offloading. It additionally provides local area wireless communication to interface with other nearby core stages, payloads, cameras, and other noncritical components. It may also serve as a backup link to critical vehicle subsystem components.

The command and data handling system leverages development from the Orion program. It includes four redundant flight control modules housed within two vehicle management computers, powered by the IBM PowerPC 750 FX processor chip. [36], [37] Also adapted from Orion is a wired network using time-triggered gigabit ethernet [36] linking the flight computers to power and data units. This network is triple-redundant and connects to other core stages across each JUMP Mating Mechanism and to the launch vehicle or payload through the dual-mode payload attach fitting. Data storage is provided by three solid state data recorders.

The imaging system consists of 36 cameras positioned to image various flight phases including launch vehicle shroud jettison, dual-mode payload attach fitting separation (from launch vehicle) and attach (to payload), core stage mating, lunar descent flight path, and lunar landing. Each camera has a 125° or greater field of view. There are six dorsal, six ventral, eighteen side mounted, four solar array mounted, and two steerable cameras mounted on the forward skirt.

The JUMP Lander GNC includes two star trackers, one optical navigation camera, three inertial measurement units, five docking cameras, and six LIDAR units. The GNC enables autonomous flight between Earth and the Moon, rendezvous and capture of the payload, and lunar descent and landing. The docking cameras and five LIDARs are aligned with the JUMP Mating Mechanisms and the dual-mode payload attach fitting. The sixth LIDAR is positioned to support landing.

*Structures and Mechanisms*

The core stage primary structure must support the load of the core stage during manufacture, transport, ground handling, testing, launch processing, CLV ascent, and orbital and transfer flight (ascent to Cislunar, Cislunar operations, Cislunar to lunar). It must support the load of the Core Stage and fractional load of the payload during lunar descent and landing. And it must support the load of the core stage, fractional load of payload, and disturbance loads from the offloading system on the lunar surface during payload offloading. It must also provide secondary structure interfaces for mounting of subsystems and components. It must further minimizes adverse transfer of thermal loads across structure and adverse impact of structural deflections on JUMP Mating Mechanisms and vehicle sensors. The primary structure design should also minimize development cost, mission risk, and manufacturing and assembly time.

The primary structures for the JUMP Lander are the intertank, forward skirt, and aft skirt. The intertank connects the two propellant tanks, houses lander subsystems, serves as the connection point for the intermediate Capture and Alignment System and JUMP Mating Mechanisms, and is the upper structural interface for the landing gear. The forward skirt is connected to the top of the oxidizer tank and the aft skirt is connected to the bottom of the fuel tank. The forward and aft skirts house the RCS thrusters and provide additional attachment points for subsystems. While the propellant tanks also carry structural loads, they are being treated as part of the propulsion system and are thus not included in the primary structure.

Described in a separate paper [38], the JUMP Mating Mechanism is the mechanical system that enables JUMP Lander core stages to be joined together. Inspired by the bolt system used to join the Space Shuttle Orbiter to the Eternal Tank, the JMM is an automated bolt system. Six JMM assemblies on each core stage drive bolts into threaded structural elements in the counterpart JMMs on another core stage. The JMMs are androgynous such that any JMM can serve as the active or passive mechanism during structural mating. Each core stage has a total of twelve JMMs in two sets. Thus, each core stage can mate to two other core stages. The JMMs are mounted to the forward skirt, intertank, and aft skirt.

The JMM relies on very precise positioning of the core stages in order for the JMM bolt on one core stage to secure to the Threaded Frame Mount [38] of the JMM on the other core stage. This is accomplished by the Capture and Alignment System (CAS).

The JUMP Lander CAS automates an EVA capability demonstrated multiple times in the Space Shuttle Program. On STS-49, spacewalking astronauts captured the stranded INTELSAT VI satellite by hand [39], physically grabbing the satellite to ease it into the payload bay for servicing.

Even before STS-49, the NASA Jet Propulsion Lab had been exploring methods to autonomously capture a satellite with twin robotic arms [40] and the Canadian Space Agency has also explored robotic satellite capture concepts [41] in laboratory testing. The Robonaut was developed at NASA Johnson Space Center as a humanoid robot capable of performing tasks too dangerous for people. [42]

The JUMP Lander CAS utilizes robotic arms inspired by Robonaut and removable EVA handrails. There is one arm and one handrail per JMM, such that the robot arm on one core stage can grasp the handrail on the other core stage. A given core stage uses six JMMs to dock with another core stage, thus twelve arms are engaged collectively to guide the two core stages into alignment and provide the initial compressive force for the JMMs to engage and perform the structural mating.

The Dual-Mode Payload Attach Fitting (DMPAF) is a ring-truss structure such as the notional fitting shown in Figure 12 used to join the core stage to the launch vehicle and payload. In addition to serving as a structural connection, the DMPAF can also transfer power and data.

The DMPAF is mounted to the top of the core stage, welded to the top of the forward skirt. The core stage is launched upside down with the DMPAF providing the structural interface to the launch vehicle upper stage. The DMPAF separates from the upper stage after upper stage main engine cutoff. After the core stages have mated, the DMPAF is used to mate to the lunar surface payload, interfacing with a corresponding adapter on the payload.

The mechanisms used to secure the DMPAF to the lunar payload and launch vehicle upper stage remain as forward work but may include options such as the JUMP Mating Mechanism or ISS Segment-to-Segment Attach System.

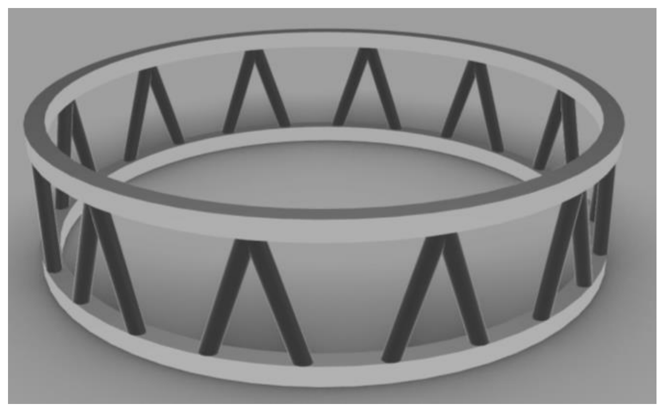

Figure 12. Notional Payload Attach Fitting

Landing legs deploy to permit the JUMP Lander to touch down on the lunar surface. The number and configuration of the legs are dependent on the number of core stages needed to land the payload. In most cases the number of landing legs will be three per core stage, with one primary leg and two secondary legs. The secondary legs will deploy to a position 1.22 meters from the core stage such that they do not interfere with the secondary legs of the adjacent core stage. The primary legs will extend 2.04 meters from the core stage to provide stability. All legs nominally deploy to half a meter beneath the main engine nozzle and are adjustable an additional two meters to allow for leveling on uneven terrain.

## 5. INTEGRATED CONCEPT ILLUSTRATION VARIANT DESIGNS

With the subsystem sizing completed the masses of the Concept Illustration Variants can be estimated and then the rocket equation can be applied to estimate their payload capacities.

*Concept Illustration Variant 1*

The lander has an estimated height of 5.67 meters. The propellant tanks are 4.2 meters in diameter and with the solar array deployed the spacecraft has a total width of 21.2 meters. Table 1 provides a mass summary for Concept Illustration Variant 1.

Table 1. Concept Illustration Variant 1 Mass Summary

| **Concept Illustration Variant 1** | **Mass (kg)** |
|---|---|
| C&DH | 75.35 |
| C&T | 64.14 |
| GN&C | 48.54 |
| Non-Prop Fluids | 153.47 |
| Power | 403.30 |
| Propellant | 10648.63 |
| Propulsion | 724.75 |
| Structures | 502.81 |
| JUMP Mating Mechanism | 977.12 |
| Thermal | 539.24 |
| Total | 14137.36 |
| | |
| Dry Mass | 3335.26 |
| Inert Mass | 3488.73 |
| Total Mass | 14137.36 |
| | |
| Program Manager’s Reserve (PMR) | 700.40 |
| | |
| Payload (Jettisonable Capture and Alignment System) | 162.24 |
| | |
| Total Vehicle Mass | 14837.76 |
| Total Launch Mass | 15000.00 |
| Inert Launch Mass | 4351.37 |

*Concept Illustration Variant 2*

The LOX-Methane lander has an estimated height of 3.79 meters. The shorter height is to be expected due to the higher density of liquid methane as contrasted with liquid hydrogen. The tank diameter is identical at 4.2 meters, but the solar array is smaller due to not having to power the fuel cell, resulting in a width of 19.65 meters with the array deployed. The mass summary is shown in Table 2.

Table 2. Concept Illustration Variant 2 Mass Summary

| **Concept Illustration Variant 2** | **Mass (kg)** |
|---|---|
| C&DH | 75.35 |
| C&T | 64.14 |
| GN&C | 48.54 |
| Non-Prop Fluids | 153.47 |
| Power | 1086.04 |
| Propellant | 9972.36 |
| Propulsion | 557.96 |
| Structures | 502.81 |
| JUMP Mating Mechanism | 977.12 |
| Thermal | 582.19 |
| Total | 14019.99 |
| | |
| Dry Mass | 3894.16 |
| Inert Mass | 4047.63 |
| Total Mass | 14019.99 |
| | |
| Program Manager’s Reserve (PMR) | 817.77 |
| | |
| Payload (Jettisonable Capture and Alignment System) | 162.24 |
| | |
| Total Vehicle Mass | 14837.76 |
| Total Launch Mass | 15000.00 |
| Inert Launch Mass | 5027.64 |

*Concept Illustration Variant 3*

Similar in height, the MMH-MON-3 lander is estimated to be 3.86 meters tall. Like the other landers, the tank diameters is 4.2 meters. With neither fuel cells nor cryocoolers to power, this variant has the smallest solar array giving the lander a width of 17.15 meters with the array deployed. The mass summary is shown in Table 3.

Table 3. Concept Illustration Variant 3 Mass Summary

| **Concept Illustration Variant 3** | **Mass (kg)** |
|---|---|
| C&DH | 75.35 |
| C&T | 64.14 |
| GN&C | 48.54 |
| Non-Prop Fluids | 153.47 |
| Power | 927.19 |
| Propellant | 10263.02 |
| Propulsion | 556.96 |
| Structures | 502.81 |
| JUMP Mating Mechanism | 977.12 |
| Thermal | 501.83 |
| Total | 14070.43 |
| | |
| Dry Mass | 3653.94 |
| Inert Mass | 3807.41 |
| Total Mass | 14070.43 |
| | |
| Program Manager's Reserve (PMR) | 767.33 |
| | |
| Payload (Jettisonable Capture and Alignment System) | 162.24 |
| | |
| Total Vehicle Mass | 14837.76 |
| Total Launch Mass | 15000.00 |
| Inert Launch Mass | 4736.98 |

*Estimated Lander Performance*

A delta-v of 2.73 km/s is used as the change in velocity required for the JUMP lander to deliver payload from Cislunar space to the lunar surface. Calculations based on the rocket equation, Equation 1 below, and this delta-v can estimate the payload mass that each Concept Illustration Variant can deliver to the lunar surface.

$$\Delta V = I_{SP} g_o ln \frac{m_o}{m_f}$$

Equation 1. The Rocket Equation

Single Core Delivery

The performance obtained if the core stage is only mated to a payload and is not joined with other core stages sets a baseline level of performance that can be compared with traditional lunar landers.

Concept Illustration Variant 3, the monomethyl hydrazine / nitrogen tetroxide lander, has the lowest performance and is only able to deliver 2687 kg to the lunar surface. The liquid oxygen / liquid methane lander, Concept Illustration Variant 2, has only slightly better performance. It delivers 2330 kg to the surface. For all practical purposes, the two are roughly equal, which is to be expected based on the relatively low specific impulse of the Morpheus HD4 engine used in Concept Illustration Variant 2. The liquid oxygen / liquid hydrogen JUMP Lander offers significantly better performance and can land 8719 kg on the Moon.

Common Habitat Delivery

The JUMP approach enables these core stages to deliver multiples of their payload capacity. While the Common Habitat design effort is still preliminary and has not established a mass, it has established a target mass of roughly 30 tons to represent a partially offloaded Common Habitat. With the JUMP Lander goal being a 30-ton capability, the rocket equation can then be used to identify the number of core stages that would need to be joined together to deliver an ~30-ton Common Habitat.

For Concept Illustration Variant 3, eleven core stages can deliver a 29.56-ton payload. Nine cores can deliver a 24.19-ton payload and thirteen cores deliver a 34.93-ton payload.

For Concept Illustration Variant 2, thirteen core stages can deliver a 30.29-ton payload. Eleven cores can deliver a 25.63-ton payload and fifteen cores deliver a 34.96-ton payload.

For Concept Illustration Variant 1, four core stages can deliver a 34.88-ton payload. Three cores can deliver a 26.16-ton payload and five cores can deliver a 43.6-ton payload.

*JUMP Lander Concept Extensibility*

The Concept Illustration Variants are high level paper studies intended primarily to show the feasibility of the JUMP concept. The concept itself can be extended to any number of lander systems.

In particular, the concept can be used by any of the NASA HLS providers. In the case of the Blue Federation or Dynetics landers, the concept can be applied directly to operate essentially in the same manner described in this paper. In the case of Starship, a similar approach could be applied, but given that Starship already has a lunar surface payload capacity of 100 tons this would only be necessary if a payload in excess of that mass were to be introduced to an architecture. It is conceivable that such a payload could exist in a lunar colonization scenario, but probably not in the Artemis program. However, the JUMP Mating Mechanism could be utilized by Starship to support mating for in-space refueling.

A smaller version of the JUMP concept could also be applied to NASA CLPS landers. For instance, two Astrobotic Peregrine landers (~265 kg capacity each) could use a JUMP approach to land a 500 kg payload on the Moon.

## 6. Forward Work

As it stands, the LOX-Hydrogen JUMP Lander configuration is clearly the preferred configuration. For the mission that motivated this study – delivery of a Common Habitat to the lunar surface – it appears that either three or four core stages, depending on design refinement, can land the Common Habitat on the Moon.

Use of a tug may be explored as a method to increase payload capacities. This approach was baselined in the NASA reference concept for the Artemis crew lander and is being pursued by the Blue Federation commercial crew lander.

Continued design refinement of lander subsystems and components will help to improve the fidelity of lander masses. In many cases, mass estimates are conservative and design refinement may reveal performance gains. However, some fidelity improvements may uncover mass threats.

Engine selection also negatively impacted lander performance as the engines with publicly available data were not necessarily the optimal engines for lunar landers – there has been no cause for industry to develop lander engines. There is likely little room for improvement in hypergolic engines. While substantial improvement might be achieved with a more appropriately sized methane engine than the Morpheus main engine, it does not appear that methane will trade favorably under any conceivable $I_{sp}$. The best gains are likely to be found in a LOX-Hydrogen engine with similar $I_{sp}$ but lower mass than the RL-10.

Several of the mechanisms employed on the JUMP Lander were mentioned at only a high level. Additional design effort is needed to refine the integrated solar array and radiator wing. The Capture and Alignment System, Dual-Mode Payload Attachment Fitting, and landing gear will all benefit from additional design effort. Another planned activity is to fabricate a prototype JUMP Mating Mechanism as part of an effort to further refine the concept.

Finally, a future investigation should develop a reference mission for the specific case of delivering the Common Habitat to the lunar surface.

## Acknowledgements

The authors would like to thank all lunar lander teams who have supported various NASA studies over the years, including the Altair project, Morpheus team, Mighty Eagle team, NASA and industry partner HLS teams, and the many pre-program study teams who all created options the nation could consider for a human return to the Moon.

## References

[1] Artemis, Humanity's Return to the Moon, https://www.nasa.gov/specials/artemis/, accessed September 4, 2020.

[2] Hautaluoma, Grey, Commercial Lunar Payload Services Update, https://www.nasa.gov/feature/commercial-lunar-payload-services-update, accessed September 4, 2020.

[3] Foust, Jeff, Masten wins NASA lunar lander award, https://spacenews.com/masten-wins-nasa-lunar-lander-award/, accessed September 4, 2020.

[4] Astrobotic, Astrobotic Awarded $199.5 Million Contract to Deliver Nasa Moon Rover, https://www.astrobotic.com/2020/6/11/astrobotic-awarded-199-5-million-contract-to-deliver-nasa-moon-rover, accessed September 4, 2020.

[5] SpaceX, Starship Users Guide Revision 1.0, https://www.spacex.com/media/starship_users_guide_v1.pdf, accessed September 4, 2020.

[6] The Altair Lunar Lander, Constellation Program: America's Spacecraft for a New Generation of Explorers, NASA Facts, https://www.nasa.gov/pdf/289914main_fs_altair_lunar_lander.pdf, accessed September 4, 2020.

[7] Howard, Robert, Opportunities and Challenges of a Common Habitat for Transit and Surface Operations, IEEE Aerospace Conference, IEEE, Big Sky, MT, 2019.

[8] Howard, Robert, A Permanent Human Lunar Surface Presence Enabled By a CLV Class JUMP Lander, AIAA Propulsion and Energy Forum, AIAA, Indianapolis, IN, 2019.

[9] Howard, Robert, A Joinable Undercarriage to Maximize Payload (JUMP) Lunar Lander for Cargo Delivery to the Lunar Surface, AIAA Propulsion and Energy Forum, AIAA, Indianapolis, IN, 2019.

[10] Aerojet Rocketdyne, RL10 Propulsion System, https://www.rocket.com/sites/default/files/documents/Capabilities/PDFs/RL10_data_sheet.pdf, accessed September 12, 2020.

[11] Mechler, John, Morehead, Robert, Combustion Stability Characteristics of the Project Morpheus Liquid Oxygen / Liquid Methane Main Engine, AIAA/ASME/SAE/ASEE Joint Propulsion Conference, July 2014.

[12] Morehead, Robert, Project Morpheus Main Engine Development and Preliminary Flight Testing, 47th AIAA Joint Propulsion Conference, July 2011.

[13] Orbital Maneuvering Systems Overview, https://spaceflight.nasa.gov/shuttle/reference/shutref/orbiter/oms/overview.html, accessed September 12, 2020.

[14] Integrated Vehicle Fluids, United Launch Alliance, https://patents.google.com/patent/US20120227374A1/en, accessed September 13, 2020.

[15] Aerojet Rocketdyne, In-Space Propulsion Data Sheets, https://www.rocket.com/sites/default/files/documents/In-Space%20Data%20Sheets%204.8.20.pdf, accessed September 12, 2020.

[16] Calvignac, Jacky, Dang, Lisa, Tramel, Terri, Paseur, Lila, Design and Testing of Non-Toxic RCS Thrusters for Second Generation Reusable Launch Vehicle, 39th AIAA/ASME/SAE/ASEE Joint Propulsion Conference and Exhibit, Huntsville, AL, July 2003.

[17] Brown, Thomas, Klem, Mark, McRight, Patrick, Foundational Methane Propulsion Related Technology Efforts, and Challenges for Applications to Human Exploration Beyond Earth Orbit, Space Propulsion 2016, Rome, Italy, May 2016.

[18] McManamen, J. Patrick, Hurlbert, Eric A., Kroeger, Dennis J., Development and Flight Operation of a 5 lbf to 20 lbf O2/CH4 Roll Control Engine for Project Morpheus, AIAA Propulsion and Energy Forum, Cleveland, OH, 2014.https://arc.aiaa.org/doi/pdf/10.2514/6.2014-3589, accessed September 12, 2020.

[19] Oleson, Steven, Dankanich, John, Grantier, David, Martini, Mike, Warner, Joe, Williams, Glenn L., Schmitz, Paul, Colozza, Anthony, Fittje, James, Packard, Thomas, Gyekenyesi, John, A Kuiper Belt Object Orbiter Enabled by 10 kW Kilopower Electric Propulsion, AIAA Propulsion and Energy Forum, AIAA, Indianapolis, IN, 2019.

[20] Colozza, Anthony, Small Lunar Base Camp and in Situ Resource Utilization Oxygen Production Facility Power System Comparison, NASA/CR-2020-220368, NASA Glenn Research Center, March 1, 2020.

[21] Gibson, Marc and Schmitz, Paul, Higher Power Design Concepts for NASA's Kilopower Reactor, IEEE Aerospace Conference, IEE, Big Sky, MT, 2020.

[22] Warshay, Marvin, Prokopius, Paul, The Fuel Cell in Space: Yesterday, Today and Tomorrow, NASA Technical Memorandum 102366, Grove Anniversary (1839-1989) Fuel CEll Symposium, 1989.

[23] Fitzgerald, Justin, O'Bryan, Nancy, Fuel Cells: A Better Energy Source for Earth and Space, https://www.nasa.gov/centers/glenn/technology/fuel_cells.html, accessed September 4, 2020.

[24] GS Yuasa Corporation, GS Yuasa Receives Lithium-ion Battery Order for International Space Station, https://www.gs-yuasa.com/en/newsrelease/pdf/20121130e.pdf, accessed September 4, 2020.

[25] Z4J Space Solar Cell, SolAero Technologies, https://solaerotech.com/wp-content/uploads/2019/04/Z4J-Datasheet-April-2019-10.pdf, accessed September 5, 2020.

[26] Salazar, Sean Louis, NASA gives contract to SolAero for Gateway project, Z6 Magazine, August 24, 2019, https://z6mag.com/2019/08/24/nasa-gives-contract-to-solaero-for-gateway-project/, accessed September 5, 2020.

[27] Plachta, D.W., Christie, R.J., Carlberg, E. , Feller, J.R., Cryogenic Propellant Boil-Off Reduction System , AIP Conference Proceedings 985, 1457, 2008.

[28] LOX/Methane Gap Assessment Report, International Agency Working Group, https://www.globalspaceexploration.org/wordpress/docs/Lox%20Methane%20Gap%20Assessment%20Report.pdf, accessed September 14, 2020.

[30] Burke, Kenneth, Fuel Cells for Space Science Applications, AIAA First International Energy Conversion Engineering Conference, Portsmouth, VA, August 2003.

[31] Larminie, James, Dicks, Andrew, Fuel Cell Systems Explained Second Edition, John Wiley & Sons, 2003.

[32] QLC-1000 PEM Electrolyzer Cell Stack, Fuel Cell Store, https://www.fuelcellstore.com/pem-electrolyzer-cell-stack-qlc-1000, accessed September 7, 2020.

[33] Active Thermal Control System (ATCS) Overview, https://www.nasa.gov/pdf/473486main_iss_atcs_overview.pdf, accessed September 9, 2020.

[34] Wang, Xiao-Yen J., Yuko, James R., Thermal Performance of Orion Active Thermal Control System With Seven-Panel Reduced-Curvature Radiator, Thermal and Fluids Analysis Workshop (TFAWS), NASA Engineering Safety Center, Houston, Texas, August 2010.

[29] Orion Explore Farther Media Kit, European Space Agency, http://esamultimedia.esa.int/docs/HRE/Orion_ExploreFarther-mediakit.pdf, accessed September 7, 2020.

[35] Mallett, Ian, Space Calc, https://space.geometrian.com/calcs/radiators.php, accessed September 9, 2020.

[36] Cichan, Timothy, Timmons, Kerry, Coderre, Kathleen, Pratt, William, The Orion Spacecraft as a Key Element in a Deep Space Gateway, https://www.lockheedmartin.com/content/dam/lockheed-martin/eo/photo/webt/Orion-Spacecraft-as-a-Key-Element-to-Deep-Space.pdf, accessed August 29, 2020.

[37] Cole, Sally, Orion Spacecraft's Avionics Designed for Reliability in Deep Space, Military Embedded Systems, http://mil-embedded.com/articles/orion-avionics-designed-reliability-deep-space/, accessed August 29, 2020.

[38] Howard, Robert, An Initial Concept for a JUMP Mating Mechanism, AIAA ASCEND Conference, AIAA, Virtual Conference, 2020.

[39] NASA, Space Shuttle Mission Archives: STS-49, https://www.nasa.gov/mission_pages/shuttle/shuttlemissions/archives/sts-49.html, accessed September 1, 2020.

[40] Wilcox, Brian, Tso, Kam, Litwin, Todd, Hayati, Samad, Bon, Bruce, Autonomous Sensor-Based Dual-Arm Satellite Grappling, https://ntrs.nasa.gov/api/citations/19900020493/downloads/19900020493.pdf, accessed September 1, 2020.

[41] Rekleitis, Ioannis, Martin, Eric, Rouleau, Guy, L'Archevêque, Régent, Parsa, Kourosh, Dupuis, Eric, Autonomous Capture of a Tumbling Satellite, https://onlinelibrary.wiley.com/doi/pdf/10.1002/rob.20194, accessed September 1, 2020.

[42] Robonaut, https://robonaut.jsc.nasa.gov/R2/, accessed September 1, 2020.

## BIOGRAPHY

Robert Howard is the Habitability Domain Lead in the Habitability and Human Factors Branch and co-lead of the Center for Design and Space Architecture at Johnson Space Center in Houston, TX. He leads teams of architects, industrial designers, engineers and usability experts to develop and evaluate concepts for spacecraft cabin and cockpit configurations. He has served on design teams for several NASA spacecraft study teams including the Orion Multi-Purpose Crew Vehicle, Orion Capsule Parachute Assembly System, Altair Lunar Lander, Lunar Electric Rover / Multi-Mission Space Exploration Vehicle, Deep Space Habitat, Waypoint Spacecraft, Exploration Augmentation Module, Asteroid Retrieval Utilization Mission, Mars Ascent Vehicle, Deep Space Gateway, as well as Mars surface and Phobos mission studies. He received a B.S. in General Science from Morehouse College, a Bachelor of Aerospace Engineering from Georgia Tech, a Master of Science in Industrial Engineering with a focus in Human Factors from North Carolina A&T State University, and a Ph.D. in Aerospace Engineering with a focus in Spacecraft Engineering from the University of Tennessee Space Institute. He also holds a certificate in Human Systems Integration from the Naval Postgraduate School and is a graduate of the NASA Space Systems Engineering Development Program.

Nehemiah Williams serves as the Integrated Vehicle Performance lead in the Orion Program's Vehicle Integration Office (VIO) where his primary responsibilities include verifying the functional capabilities of the Orion spacecraft's integrated sub-systems (e.g. propulsion, thermal, life support systems and power) and communicating vehicle performance to mission planners in support of Project Artemis, NASA's lunar exploration initiative. Nehemiah entered full time civil service at NASA's Johnson Space Center (JSC) in 2016, working initially as a liquid propulsion systems engineer, where he supported reaction control and small scale rocket engine test campaigns, reaction control thruster thermal model development and multi-phase computational fluid dynamics analysis of rocket engine injection systems in the Propulsion and Power Division at JSC. Nehemiah's higher education includes B.S. degrees in Biblical Studies from Philadelphia Biblical University in Langhorne, Pennsylvania (2004) and Mechanical Engineering from Temple University in Philadelphia, Pennsylvania (2008) and both an M.S. and a Ph.D. in Aerospace Engineering, each from the University of Tennessee Space Institute in Tullahoma, Tennessee (2010, 2016).

Sarosh Nandwani is a Human/Machine Systems Engineer on the Orion Human Engineering team at Johnson Space Center in Houston, TX. She coordinates and supports human-in-the-loop tests, collects and analyzes data, and develops and reviews verifications for various requirements of the Orion vehicle's human systems requirements. Previously, she has worked at the Neutral Buoyancy Lab as a Pathways co-op and as a Program Integration intern with the NASA contractor, Barrios Technology Ltd. Prior to graduating, she also interned with a medical device lab on campus and an oil and gas company. She graduated from the University of Texas at Austin with a Bachelor's of Science in Mechanical Engineering and a Bachelor's of Arts in Anthropology Honors.